Molecular Crystals and Liquid Crystals
Publication details, including instructions for authors and subscription information:
http://www.tandfonline.com/loi/gmcl16

Analogy Between Hydrodynamic Instabilities in Nematic Liquid Crystal and Classical Fluid

K. Hirakawa [a] & S. Kai [a]
[a] Department of Electronics, Kyushu University, Fukuoka, 812, Japan
Version of record first published: 21 Mar 2007.

To cite this article: K. Hirakawa & S. Kai (1977): Analogy Between Hydrodynamic Instabilities in Nematic Liquid Crystal and Classical Fluid, Molecular Crystals and Liquid Crystals, 40:1, 261-284

To link to this article: http://dx.doi.org/10.1080/15421407708084489

Mol. Cryst. Liq. Cryst., 1977, Vol. 40, pp. 261–284

Printed in Holland

Analogy Between Hydrodynamic Instabilities in Nematic Liquid Crystal and Classical Fluid

K. HIRAKAWA and S. KAI
Department of Electronics, Kyushu University, Fukuoka 812, Japan

(*Received October 13, 1976; in final form December 3, 1976*)

The flow patterns formed by the electrohydrodynamic effect of the nematic liquid crystal are observed. It is found that the phase diagram made from the observation bears a strong resemblance to that of isotropic fluid. The typical patterns observed under the variable frequency and voltage are shown.

1 INTRODUCTION

It is well known for an isotropic fluid that as an applied external stress increases, the system changes from a laminar flow into turbulent flow. An example is the Benard–Rayleigh problem. When a horizontal layer of fluid is heated from below, at a critical temperature gradient a regularly aligned roll pattern appears. With further increase of gradient, the system develops finally into turbulent flow after passing through a few transitions. Comprehensive experimental studies of this problem have been carried out, for example, by Krishnamurti.[1] On the other hand, McLaughlin and Martin,[2] using the Ruelle–Takens' theory, proposed theoretically that a non-periodic flow occurs after three or four bifurcations. The study of these sorts of hydrodynamic instabilities is very interesting from the viewpoint of statistical hydrodynamics far from thermal equilibrium.[3]

The same kinds of instabilities appear in a nematic liquid crystal.[4] Comprehensive theoretical and experimental studies of an electrohydrodynamic instability have been made by the Orsay Liquid Crystal Group. When the external stress, the voltage, is applied to a liquid crystal layer, a roll pattern named the Williams domain appears at a critical voltage in a low frequency region. On the other hand, in a high frequency region a different pattern, called the chevron texture, is formed.[5] With further increase of voltage, these

patterns change into the dynamic scattering mode, which is turbulent flow. This phenomenon is of fascinating interest in the study of hydrodynamics.

We have studied this phenomenon from the viewpoint of hydrodynamics far from thermal equilibrium.[6] At present our interests focus mainly on the following problems:

(1) the number of dissipative structures which appear, (2) preparation of a phase diagram, (3) the number of bifurcations, (4) the property of the bifurcations, (5) the analogy to the second order phase transition in a thermal equilibrium system.

The dissipative structures and the phase diagram obtained by changing the voltage and the frequency have been reported.[7,8] In those papers we have concluded from the comparison with the Krishnamurti's phase diagram that the voltage corresponds to the Rayleigh number and the inverse of the frequency corresponds to the Prandtl number after the non-dimensionalization. We have emphasized in our works that the electrohydrodynamic effect is a very advantageous example for study of hydrodynamics far from thermal equilibrium. The number and the properties of bifurcations have been studied experimentally through the fluctuation of the transmission of light and an analogy to the second order phase transition in a thermal equilibrium system has been pointed out. These results are described elsewhere.[6,9]

More recently we have made efforts to obtain more precise observation of flow patterns. In this paper, the newly classified patterns and the phase diagrams are reported. The justification of the present results is well supported by other experimental results.[10]

2 EXPERIMENTAL

In the present study, the nematic liquid crystal MBBA (*p*-methoxybenzylidene-*n*-*p'*-butylaniline) is used. As is well known, this crystal shows a nematic mesophase between $17 \sim 49°C$. Specimens with various purities were prepared, with electric conductivities ranging between 2×10^{-11} and $5 \times 10^{-10}\ \Omega^{-1}\text{cm}^{-1}$. Two kinds of cells were used for observation; one was used to observe the plane figure and the other the transverse figure. The constitution of the cells has been described elsewhere:[8] the thickness of the cells is in the range $6 \sim 10^3\ \mu\text{m}$. In the case of transverse observation the separation of electrodes is in the range of $200 \sim 300\ \mu\text{m}$. Voltages, $0 \sim 200$ volt and 20 Hz $\sim$ 2 kHz, are applied. The patterns and the flow figures were observed visually by a microscope with crossed nichols.

3 RESULTS AND DISCUSSIONS

The dissipative structure depends strongly on the strength of the external forcing parameters, especially the intensity and the frequency of the applied

voltage. In this paper, the voltage V and the frequency f are non-dimensionalized through the electric Rayleigh number $k = V/V_c \propto \sqrt{R/R_c}$ and the electrical Prandtl number $P = f_c/f$.[11] Here V_c and f_c are the critical values at which the Williams domain (roll pattern), and the chevron texture, respectively, appear, and R is the Rayleigh number.

The patterns newly classified in the present study are as follows: the arrow shows an increase of voltage.

1) $P > 1$ ($f < f_c$):

   WD → FWD → GP → quasi-GP → DSM-like → DSM1 → DSM2,

2) $P \sim 1$ ($f \sim f_c$):

   PWD → CV-like (FWD) → GP-like → DSM-like → DSM1 → DSM2,

3) $P^* < P < 1$ ($f_c < f < f^*$):

   (FWD) → CV(A) → DSM-like → DSM1 → DSM2

   for the low purity specimen,

   FWD (CV-like) → GP-like → DSM-like → DSM1 → DSM2

   for the high purity specimen,

4) $P^{**} < P < P^*$ ($f^* < f < f^{**}$):

   WP → PWP1 (CV(B)1) → PWP2 (CV(B)2) → (DSM1, DSM2)

   for the low purity specimen,

   CV(B)1 → CV(B)2 → (DSM1, DSM2)

   for the high purity specimen: in this region we call the P^*-point the CV(B)-point,

5) $P < P^{**}$ ($f > f^{**}$):

   no-stationary pattern → DSM.

The abbreviations used are as follows: WD; the Williams domain, FWD; the fluctuating Williams domain, GP; the grid pattern, DSM; the dynamic scattering mode, PWD; the propagating Williams domain, CV; the chevron texture, WP; the wavy pattern, PWP; the propagating wavy pattern. Here f_c, f^* and f^{**} are the critical frequencies at which the PWD (or CV), the WP and no-stationary pattern, respectively, appear. Figures 1(a) and 1(b) show the newly obtained phase diagrams for the low and the high purity specimens, respectively.

1 $P > 1$

In the lower frequency region, as the applied voltage is increased, the roll pattern WD begins to fluctuate: we call this the FWD. If the voltage is now

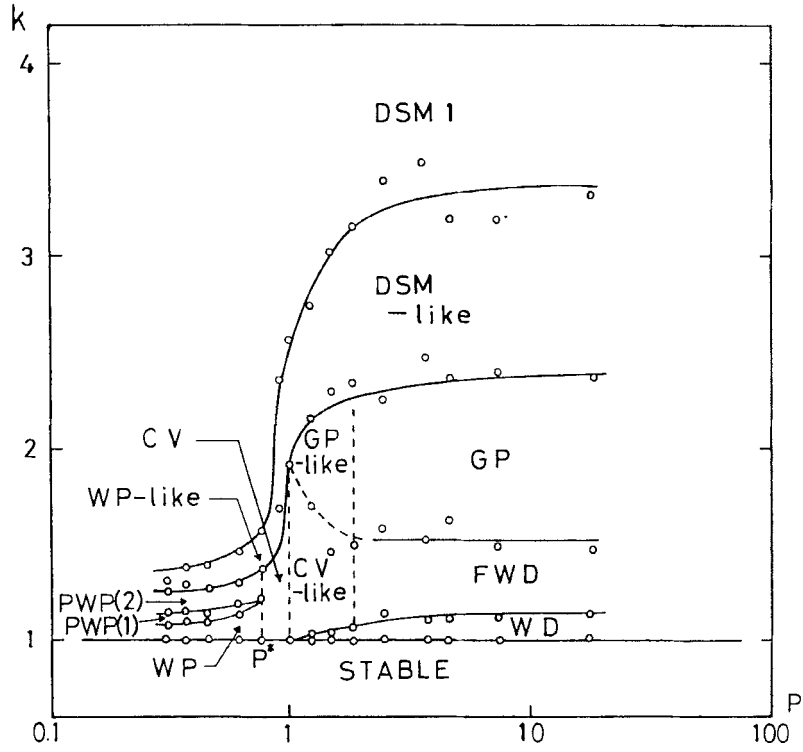

FIGURE 1(a) Phase diagram in electrohydrodynamic instabilities. For low purity specimen. Conductivity $\sigma = 2.5 \times 10^{-10}\ \Omega^{-1}\ \mathrm{cm}^{-1}$ (dc 6 volt), thickness $d = 30\ \mu\mathrm{m}$, $f_c = 380$ Hz, $f^* = 490$ Hz.

held constant, adjacent lying rolls begin to stick and break up each other and the GP, a three-dimensional steady flow, is finally formed at the GP-point k^*. The time spent in forming the GP depends on the voltage: the time decreases with increase of voltage. When the voltage is further increased, the source and the sink of flow in a grid oscillate in time; the quasi-GP is observed at k_{th}. In this region, a three-dimensional time-dependent flow appears to be formed, that is a limit cycle is formed. As the voltage approaches to the k'-point, a DSM-like flow is observed. In this region the flow seems to be a turbulent one, but a large (characteristic to flow) scale pattern is still preserved in space. At k_1 the flow becomes very complicated, and then is non-periodic. Here the spatial correlation behavior is not clear at present, but a turbulent flow region would exist above k_1: this is supported by our other experimental results.[8,12] Therefore it is concluded that after the first appearance of the limit cycle four bifurcations exist before the flow becomes turbulent.

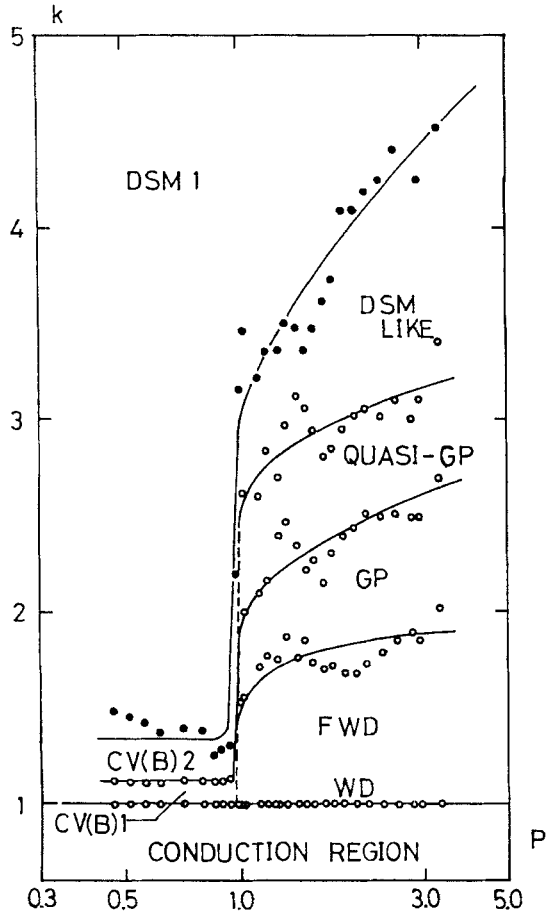

FIGURE 1(b) Phase diagram in electrohydrodynamic instabilities. For high purity specimen. Conductivity $\sigma = 2.0 \times 10^{-11}\ \Omega^{-1}\ \mathrm{cm}^{-1}$, thickness $d = 30\ \mu\mathrm{m}$, $f_c = 56$ Hz. Figures 1(a) and 1(b) are very similar to each other except for the applied frequencies. These differences of the critical frequency are caused by difference of electric conductivities. The symbols are described in detail in the text.

a) The Williams domain When a dc voltage is applied, the WD is formed at a lower critical voltage than in the case of ac voltage. An irregularly arranged mesh pattern is frequently observed. However, when the electrodes are made very homogenous, a roll pattern is formed with increase of voltage. One of the reasons that the length of a roll is short is probably the disturbance of the ordering of rolls due to the injected charge from the electrodes under the dc-field. As a result the forthcoming GP is formed at lower voltage in the dc-case, but the position where the physical quantities show anomalies lies at $k \sim 1.6$ in both dc and ac-cases.[8]

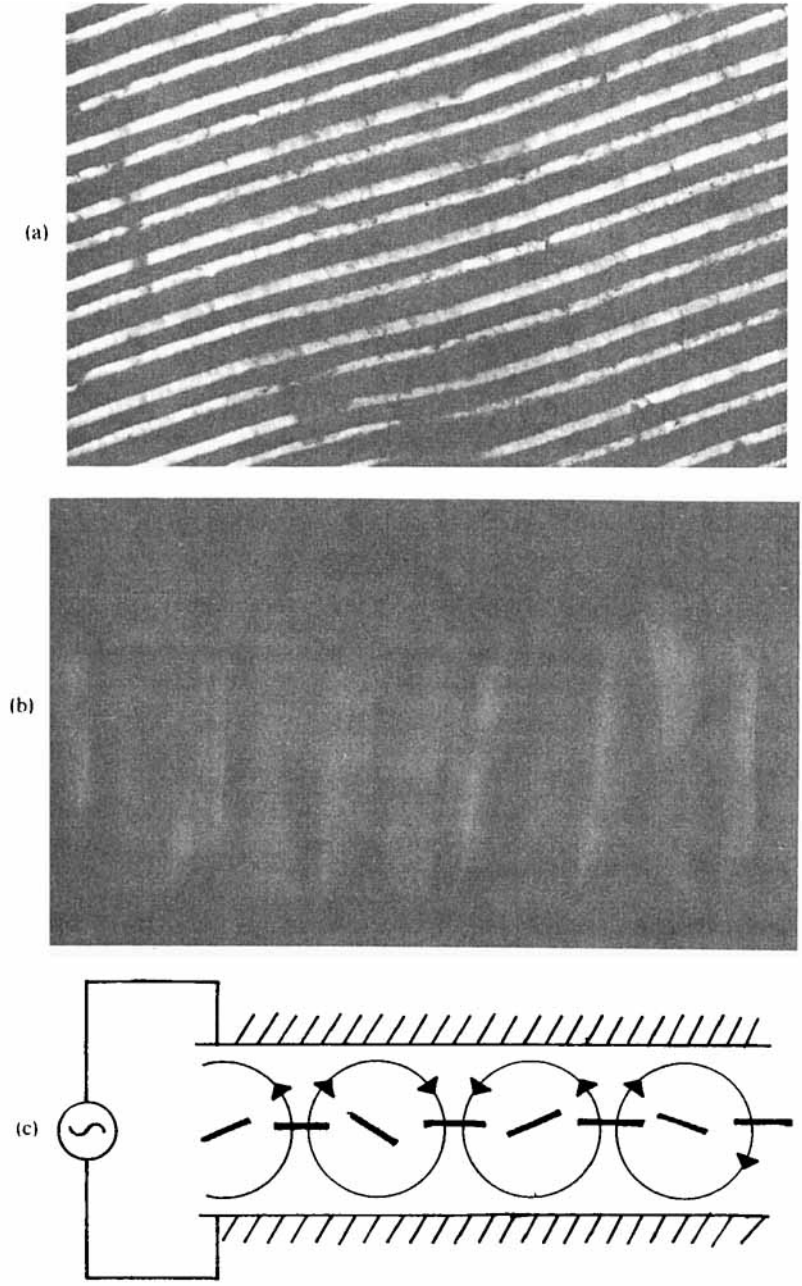

FIGURE 2 Photographs of the WD. (a) Plane figure. (b) Transverse figure. (c) Schematic figure of flow and director arrangement in liquid crystal thin cell.

On the other hand, when an ac voltage is applied the critical voltage V_c ($7 \sim 8$ volt) at which the WD appears is higher than that in the case of dc. In the case of ac, the rolls align regularly as shown in Figure 2(a). The transverse figure is shown in Figure 2(b). The value of V_c depends generally on the purity of the specimen; V_c is higher in a lower conductivity specimen. The flow and the order of the liquid crystal in the cell are shown in Figure 2(c). Regions of the crystal form lenses because of the anisotropic refractive index, thus we can see an alternative alignment of bright and dark lines. In visual observations, a nematic liquid crystal has a very advantageous point that it is not necessary to mix in other materials such as fine particles of aluminium or smoke as in the case of other fluids.

The formation time T_f of the WD is related to k as $d/T_f \propto (k-1)^{1.00 \pm 0.20}$ where d is the thickness of the cell. Since d/T_f has a dimension of velocity, it is considered that within the formation time the direction of the director becomes stable during one period of convection in the cell. In other words, it shows the voltage dependence of growth rate in the velocity fluctuation with some wave number. The same tendency is seen in the fluctuation period of the FWD and the formation time of the GP.

b) The fluctuating WD When the voltage is further increased in the WD region, where only one definite wave number grows fastest among many wave numbers, the expansion of the wave number space results in a depressing of the probability of selection of that wave number, Therefore, the growth of other wave numbers increases to be comparable with that which characterizes the WD region; the rolls begin to fluctuate. We call this the fluctuating Williams domain FWD; the plane figure is schematically shown in Figure 3.

The adjacent lying rolls stick, but after a definite time, the fluctuation time, they separate and the initial rolls are recovered: this change in time occurs over the whole range of the cell. At those intersecting points, extremely large viscous dissipation should exist. At this point, very sharp and large fluctuations of velocity occur temporarily through the combination of two vortices. Following the increase of voltage, an amount of injected energy overwhelms the energy possibly dissipated by the structuralization of WD, then an instability occurs. In order to resist this instability, the system would form fluctuations with counterwise convections through the fluctuation of rolls. Therefore, it is considered that the region of the FWD is the transition region from the WD to the forthcoming GP. In this region the fluctuation (the oscillating mode) seems to propagate along the roll axis.

The fluctuation is caused by growth of the twisted mode related to the elastic constant K_{22}.[13] The fluctuation time T_F is related with k as

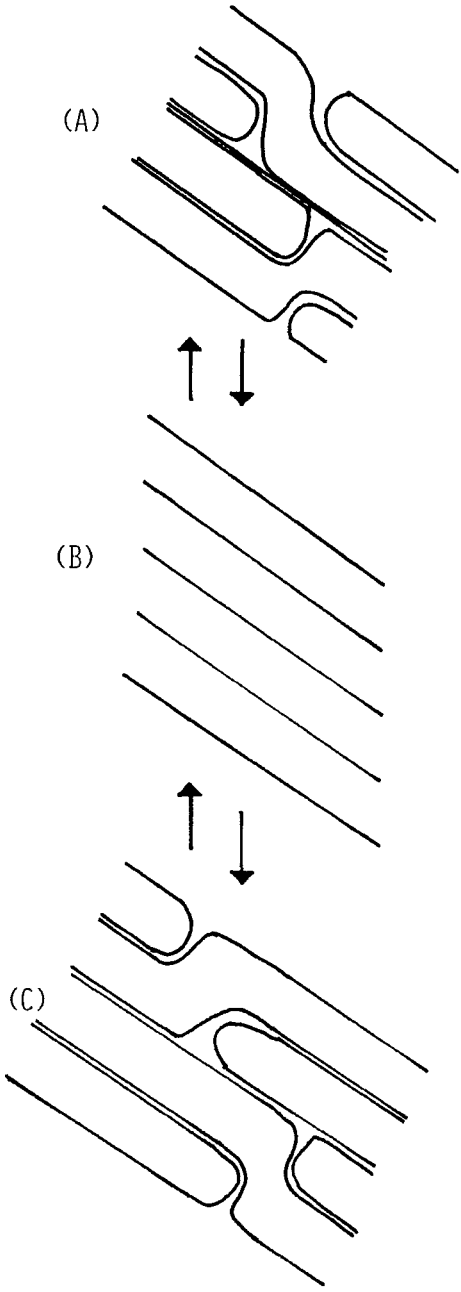

FIGURE 3 The schematic figure of the FWD. This figure shows intersecting points. With increase of time, the pattern changes as (A) → (B) → (C) → (B) → (A).

$T_F \propto (k-1)^{-0.95\pm0.07}$ [7,12] Since the fluctuation of the WD does not decay but continues in stationary form in a wide region of k, it is supposed that this is a new phase. When the cell thickness is less, the FWD appears at a lower voltage. In this case, a stationary WD is difficult to observe and the GP is not easily formed even if k is increased. This shows that the thickness affects strongly the formation of the WD and the GP. The GP is formed especially easily in the cells with thickness ranging 20 μm $\sim$ 50 μm. In the thinner or thicker cell the GP is easily not observed. In the cell about 6 μm-thick, no GP is formed. On the other hand, the appearance of an oscillating domain is not affected by the thickness: in the thin cell it is rather easily formed. In the FWD region, the system can not dissipate the energy, so that the transition to a new state should occur. This new state is three-dimensional flow and the pattern has been named the grid pattern by the authors.[8] In other words, this pattern is completely formed after the growth of the twisted mode has stopped.

c) The grid pattern This pattern, which was first discovered by the authors, occurs in a considerably lower dissipation process. When this pattern appears, the width of a grid is a little wider than that of a roll of the FWD just before the pattern appears. This suggests the possible existence of hysteresis at this transition point. This pattern is formed in the regions dc $< f < f_c$ and $k \sim 1.5 \sim 1.7$. The nearly square form of the pattern deforms gradually with increase of frequency and becomes indistinguishable from the chevron texture in the region $P < 1$. However, the GP is rather stationary and is formed in a short time at higher frequency for the same value of k. The pattern seen in this region is shown in Figure 4. In this region $k > k^*$, the critical value at which the GP appears, the formation time of the GP, T_f^{GP}, becomes shorter with increase of voltage; $T_f^{GP} \propto (k-1)^{-0.63\pm0.15}$. This dependence on k differs a little from that of the WD.[8]

It is noted in the GP region that the form of the GP is affected strongly by the property of oscillation before the GP is formed. For example, in the higher frequency region where the PWD appears, the form of the GP is extremely distorted. As is seen in Figure 4, it is clearly observed that an extremely regulated GP is formed when a dc and an ac voltage are applied in superposition.[8] One of the reasons is the regulation due to the electronic charge injected by applying the dc voltage. The GP is formed in cells of thickness about 20 μm $\sim$ 200 μm. In the case of thin layers, it is considered that the amount of charges effectively increases. On the other hand, in the case of a thick cell the wave number space expands to form a wider range and the GP is difficult to form. However, various anomalies of physical quantities are observed[6] at $k \sim 1.6$ in all specimens, thick and thin cells, so it is considered that the three-dimensional steady flow occurs at this point.

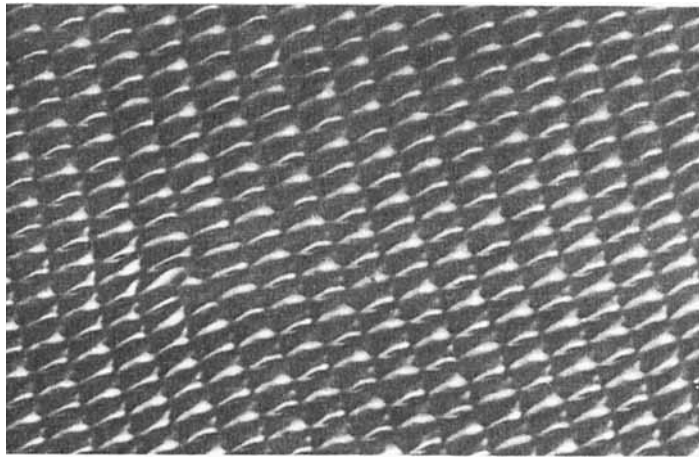

FIGURE 4 The GP ($d = 30\ \mu$m) as a dc and an ac voltage are applied in superposition.

d) The quasi-GP With further increase of voltage, where T_f^{GP} becomes independent of k, the GP begins to oscillate again (oscillating mode) and no stationary GP is formed. We call this the quasi-GP. The pattern in this region is shown in Figure 5. This pattern is apparently not greatly different from the FWD, but there is an intersection between cells: in the FWD the intersection is between rolls. Therefore, the number of oscillating points (intersecting points) is much larger than that in the FWD, and the oscillation is fast. Here a sink and a source of flow which form a cell in the GP alternate in time those of nearest neighboring GP cells. The wave number of the GP

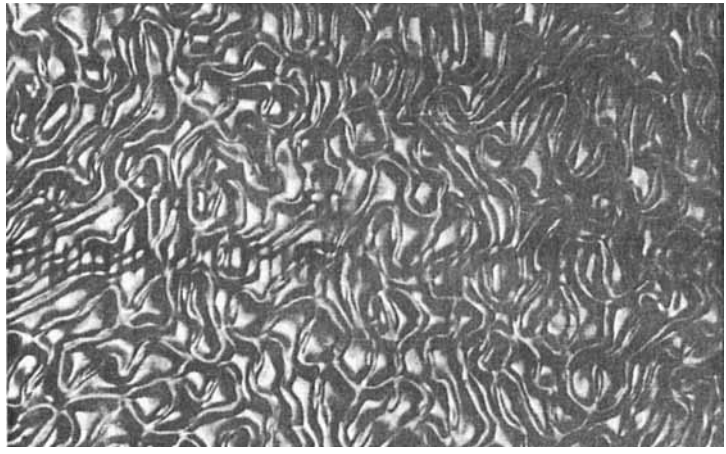

FIGURE 5 The quasi-GP. This pattern appears apparently irregular in space, as it oscillates in time.

becomes twice that of the WD; $q \sim 2/d$, where d is the roll width (or thickness of cell) of the WD. Therefore, the quasi-GP can also be called a double periodic flow. The transition point lies at k_{th}, where a limit cycle is formed: this is three-dimensional time-dependent flow.

e) The DSM-like, DSM1 and DSM2 The patterns and flows in these regions are very complicated, so that it is difficult to describe clearly the difference between these features. The DSM-like pattern which is apparently non-periodic in time seems to have some periodicity but is periodic in a considerably wide region of space. Here the periodicity in space means that the complicated flow is restricted in a macroscopic region as shown in Figure 6.

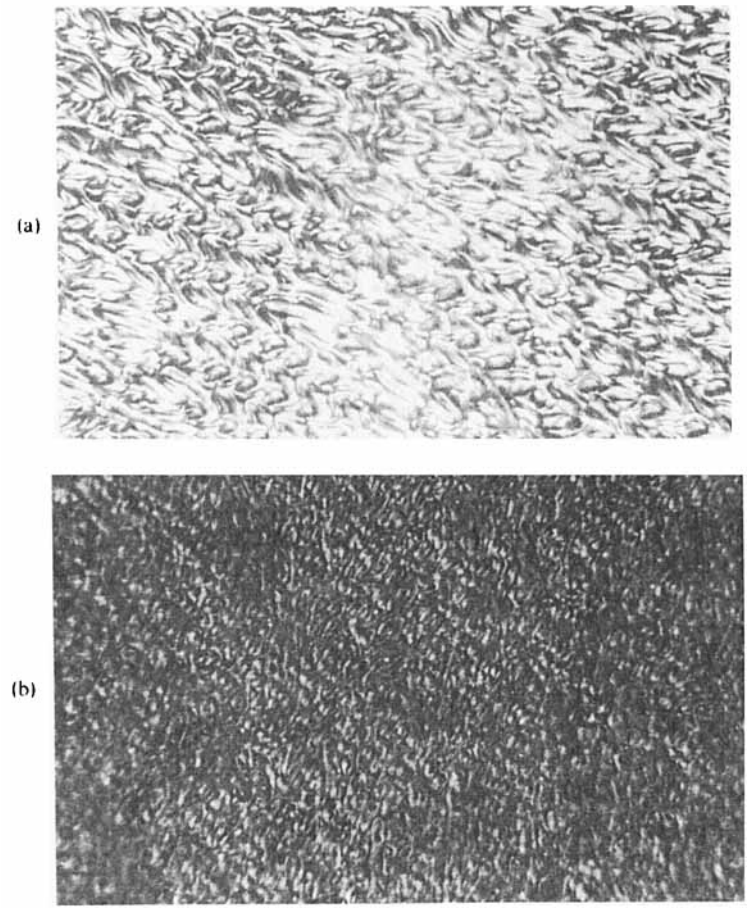

FIGURE 6 (a) The DSM-like pattern. This pattern is more complex, but may have space order. (b) The DSM1. This flow is non-periodic.

In this region, a three-dimensional time-dependent flow and a complicated limit cycle would be realized. Therefore, we observe an apparently non-periodic flow. In the DSM region, it is seen that extremely small scale flow alternates with the DSM-like flow. The flow is perfectly non-periodic in time but remains unknown in space. The difference between DSM1 and the forthcoming DSM2 is not clear in visual observation. However, the physical quantities show large anomalies at the DSM1 and DSM2 points.[6,7,12] At present we consider that the DSM2 point is the transition point to turbulent flow. No clear description can be given but the detailed behavior of patterns and flows can be observed in a movie prepared by the authors: unfortunately a description is not shown in this paper because of restriction of space.

2 $P \sim I$

When a higher frequency voltage ($f \sim f_c$) is applied, a propagation of rolls is first observed. We named this the propagating Williams domain, PWD. The direction of propagation is perpendicular to the roll axis. The groups of rolls propagate in opposite directions to each other, depending on the initial condition of the static state. This propagating aspect agrees with Busse's theory.[14] When the groups moving against each other coincide, they are missed or an opposite group is gradually overwhelmed. The same typical example is seen in open system chemical oscillations; there exists a limit cycle. The flow is probably a two-dimensional time-dependent one. When the voltage is increased at a fixed frequency, the PWD shows a similar pattern to the FWD. We may assume from the facts described above that the FWD has a limit cycle.

When k is increased further, the period of oscillation of the FWD and the number of oscillating points increase, then the rolls are torn off into pieces with the same length as the roll width; the GP-like structure is formed. In this case the form of a grid is not a square but a lozenge, where flow is considered to be three-dimensional. This change is extremely characteristic of all the cells.

The subsequently appearing pattern is the DSM-like pattern, where the GP oscillates. A distinctive feature is that the sink and the source of flow which form the GP move from place to place but the flow is not so complicated as DSM1. There exist two types of flow in the DSM-like region; one of which is the flow described just above and this pattern is called quasi-GP in the present study. The other type of flow which appears at higher voltage is more complicated. The pattern is not so regular but has some spatial order similar to the quasi-GP. The forthcoming DSM1 has a very long evolutional time and a very complicated pattern. The change into this region occurs very sharply at the instability point.

a) The propagating WD The behavior of the PWD is very interesting because of a close resemblance to the oscillating pattern of ion concentration in a chemical reaction. We can observe that an extremely slow flow occurs on a macroscopic scale already before the PWD is formed. The PWD is always observed at $P \sim 1$, independent of the purity of the specimen. The rolls form groups which propagate in an arbitrary direction, but alternate groups move in opposite directions to each other; the plane and the transverse figures seen in this region are shown in Figure 7. In Figure 7(a), some groups go upward and the other groups downward. When two groups collide, patterns disappear, forming a sink. When the groups moving in opposite directions do not collide, no roll pattern is formed in the region among them.

The propagation velocity of the PWD depends on the applied voltage, but after a little increase in voltage the PWD becomes locked in phase: the propagation of rolls comes to a halt and the FWD appears. This fact suggests that the PWD is a two-dimensional, time-dependent flow with a limit cycle. Therefore it is considered that the FWD is also a two-dimensional, time-dependent flow but with a very deformed limit cycle.

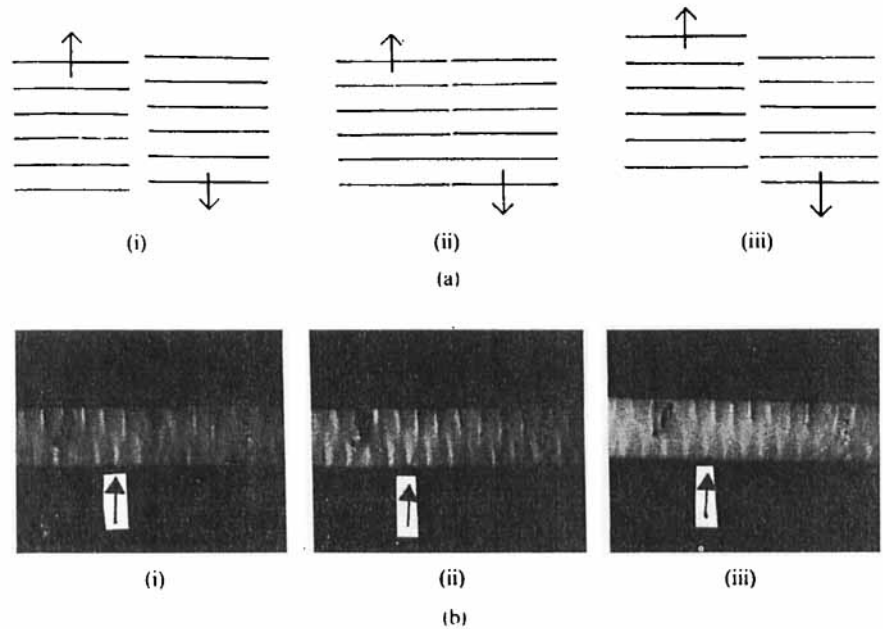

FIGURE 7 The PWD. (a) Plane figures. The propagating aspect is shown schematically for the PWD-group. (b) Transverse figures. The arrow is to show a propagating aspect. The domain is moving towards the left of the figure: (i) $t = 0$, (ii) $t = 3$, (iii) $t = 6$ sec.

b) The CV-like pattern When the voltage is increased further, the FWD becomes the CV-like pattern in which an oscillating pattern resembling the CV is seen. The CV-like pattern is clearly distinguished from the pure CV by the fact that the pattern width of CV-like is not very different from that of the WD and that there is not a discrete change from the FWD to the CV-like pattern. The CV-like pattern is shown in Figure 8.

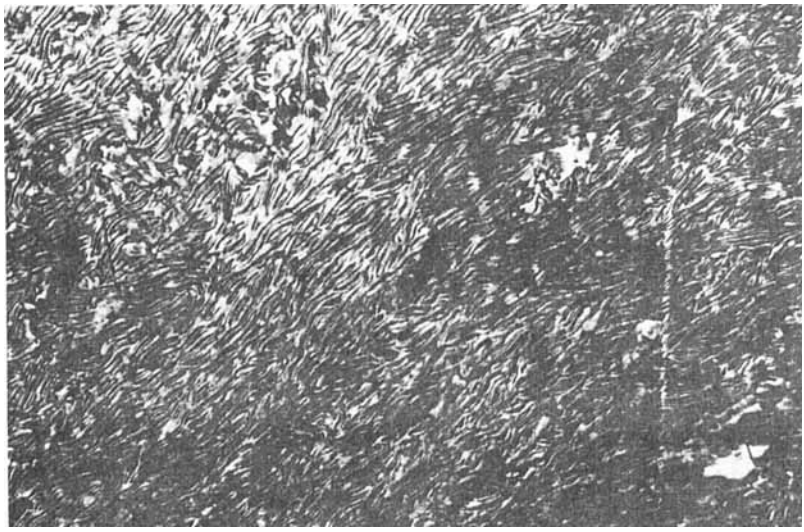

FIGURE 8 The CV-like pattern. This pattern is very similar to FWD.

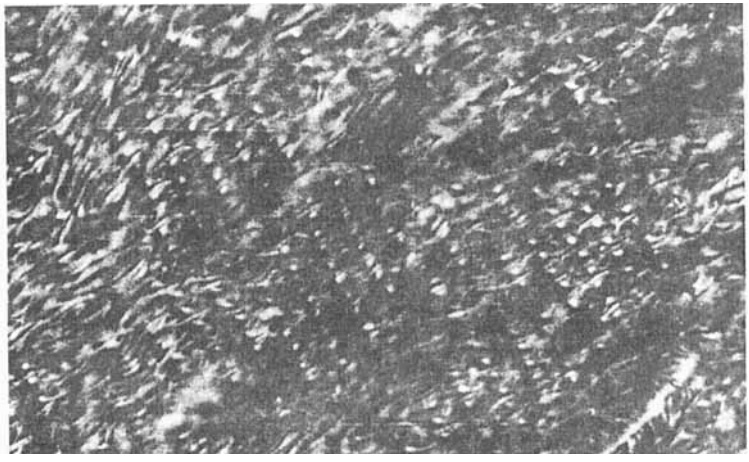

FIGURE 9 The GP-like pattern. This deformed-square pattern is stationary.

c) The GP-like pattern Holding the voltage constant for some time at a value larger than the voltage where the CV-like pattern appears, the CV-like pattern ceases to move and becomes GP-like as shown in Figure 9. This GP-like pattern has a distorted lozenge type of form but is possibly essentially no different from the GP.

d) The DSM-like pattern, DSM1 and DSM2 The forthcoming DSM-like patterns, DSM1 and DSM2 are the same as those in the region $P < 1$. The only distinct point is that in the region of the transition from DSM-like to DSM1, before the flow develops into DSM, an extremely complicated flow appears in the main mode of WD, the roll. This feature is very distinctly seen for the case $P < 1$, as shown in Figure 10.

3 $P^* < P < 1$

In this region, the oscillating pattern called the chevron texture appears at first: a limit cycle is formed. This pattern is generally divided into two classes: one is the chevron texture, CV(A), which appears in a low purity specimen or the CV-like pattern which appears in a high purity specimen for $f \lesssim f_c$ ($P \gtrsim 1$). The latter pattern resembles the CV but a fairly distinguishable point is that the roll width is of the same order as that in the WD, λ_D; about $\lambda_D/2 \sim \lambda_D/4$. Therefore this pattern apparently resembles the FWD. With increase of the voltage, the very rapidly oscillating FWD ceases to oscillate and the CV(A) is formed (Figure 11). With further increase of the voltage, the CV(A) begins to oscillate again and the DSM-like pattern is observed. However, in this region the CV(A) is hardly distinguishable from the DSM-like pattern. The appearance of the WD mode is observed during the transition from the DSM1 point to the DSM2 region.

The other class is the chevron texture CV(B) in a high purity specimen at $P < 1$. The roll width is very small; about $\lambda_D/10 \sim \lambda_D/20$. The flow has essentially the same property as that of the PWP in a low purity specimen. The pattern is divided into two classes besides the PWP following increase of voltage; CV(B)1 and CV(B)2. In the CV(B) region a cycad-leaf-like pattern is formed from the rolls; this pattern always oscillates and progressively propagates along that leaf axis. A detailed description will be given in Section 4-b, but a distinguishable point with respect to PWP is that there exists a propagation characteristic of a non-linear wave. A distinct feature in this region is that even though the PWD appears at first, as soon as the CV(B) appears the PWD completely disappears and is replaced by the CV(B); this change occurs very drastically.

As was described above, a high purity specimen has an extremely low f_c (56 Hz) and no evidence of the existence of f^* can be obtained. However,

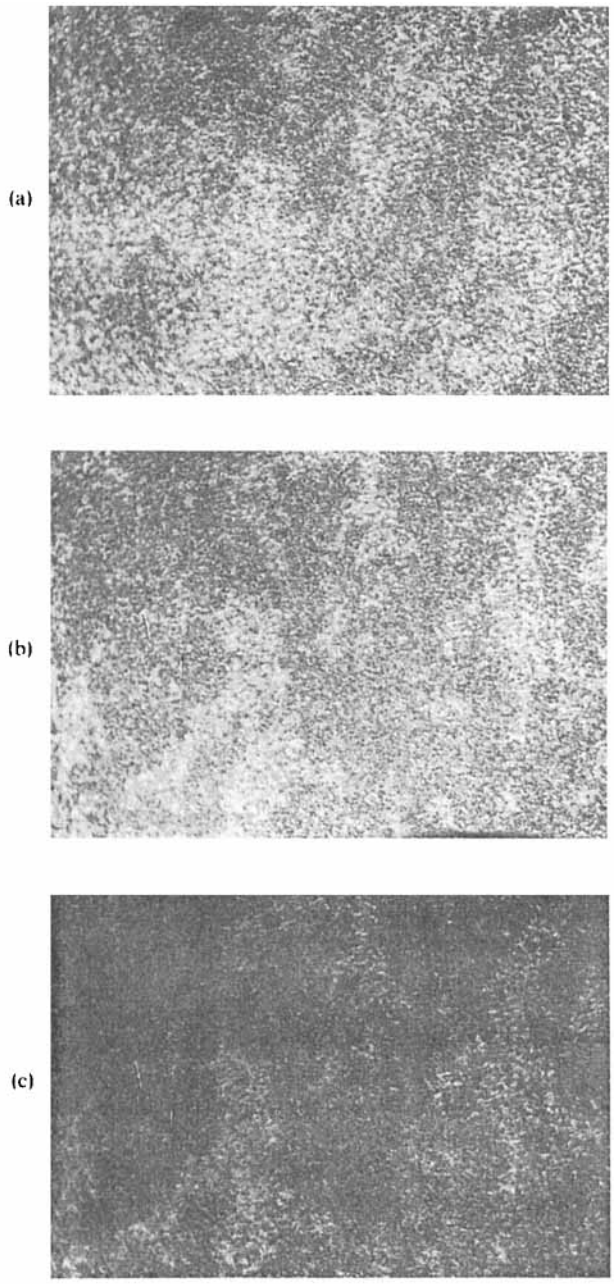

FIGURE 10 The development of DSM1. With progress of times ((a) → (b) → (c)), the DSM1 develops to fill the whole of the observed region: (i) $t = 3$, (ii) $t = 6$, (iii) $t = 9$ sec.

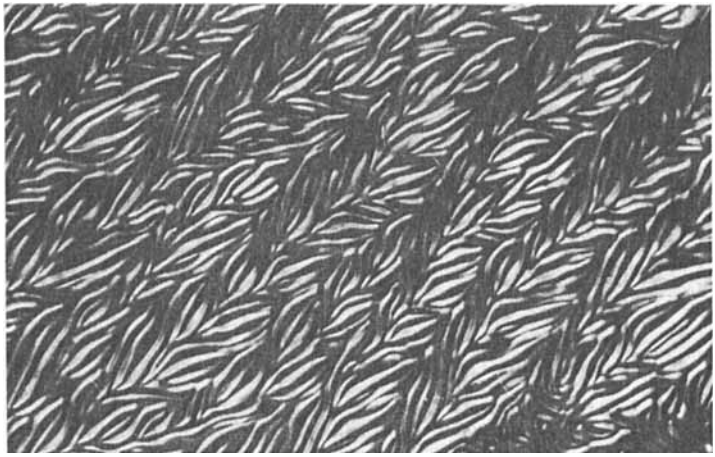

FIGURE 11 The CV(A).

from comparison with the result in the low purity specimen, it is concluded that no essential difference between PWP and CV(B) exists at $f^* < f_c$. The CV(B)2 and DSM-like patterns seen in the high purity specimen closely resemble the PWP2: the group of PWP patterns will be described in Section 4-b. We will see in a more detailed observation that the CV(B) exists in the PWP region.

4 $P^{**} < P < P^*$

In this region two types of flow are observed, depending on the purity or condition of the cell. One is the wavy roll (the wavy pattern: WP) and the other is a successive transition characterized by the appearance of the CV(B); the CV(B)1 and CV(B)2. However, the difference between them cannot be distinctly recognized. The macroscopically formed spatial structure of the CV region is easily changed into the WP pattern by external disturbance. In the CV(B) region, it is considered that the forming of the wavy-roll pattern realizes a stable pattern, but requires crossing over a considerably higher potential barrier. Which type of flow is realized is probably determined from a position in phase space which is specified by the initial condition.

Here the pattern is the dissipative structure like those in an open chemical reaction and in a low Prandtl number fluid. When a voltage is applied an instantaneous starting of flow (a very large scale flow or fluctuation of director) is seen and the wavy rolls (WP) are formed after some time. This pattern consists of sinusoidal wave-like rolls and has a double-periodic

property in space but does not move. When the voltage is increased, the sinusoidal wave-like pattern begins to propagate into a center of vortex. The velocity of the propagation increases with increase of voltage and the wavelength becomes short: we call this the PWP1.

With further increase of voltage, the width of a roll rapidly becomes small and the velocity of sinusoidal wave increases with the simultaneous decrease in wavelength, we call this the PWP2. This change in velocity has the same character as that in the transition from CV(B)1 to CV(B)2 in a high purity specimen. The voltage dependence of velocity coincides also with the cases CV(B)1 and CV(B)2. When the voltage is further increased, the flow changes into DSM, but the DSM-like pattern is difficult to observe. Therefore, probably, the flow changes directly into a non-periodic flow DSM1.

a) The WP In a low purity specimen, a wavy roll, WP, is formed. The appearance of WP at P* is very strongly affected by the contact effect between liquid crystal and cell plate; thus this pattern does not always appear every type of cell. However, it appears more frequently in a thinner cell. In this region, the dissipative structure appears in a state with a very high degree of dissipation in energy. When a voltage is applied, a flow occurs firstly on a macroscopic scale which disturbs the system over the whole range of the cell, and rolls appear gradually with increase of voltage. The rolls have only a slightly different form to the WD. With further increase of voltage, the wavy mode appears in a roll, with the propagation velocity of the wave nearly zero: we call this the wavy pattern. This pattern is shown in Figure 12(a). Here we consider that no limit cycle exists.

b) The PWP1, PWP2 and DSM When the voltage approaches the PWP1 point, the wave in a roll begins to propagate along the roll axis (Figure 12(b)). At this stage one can observe that very small rolls flow out from the wave; this corresponds probably to the CV(B)1 shown in Figure 13. The pattern next observed is the PWP2 (Figure 12(c)), corresponding probably to the CV(B)2. Here the width of the roll forming a wave decreases abruptly by about half, then the flow becomes double periodic. The propagation becomes increasingly faster with increase of voltage.[12] The next pattern appearing is a DSM-like one (Figure 12(d)), where the periodic pattern described above disappears. It is considered that the PWP1 is presumably constructed from a superposition of a small number of modes, and corresponds to the quasi-GP in the region $P > 1$.

c) The CV(B) and DSM In a high purity specimen, as the voltage approaches some value, especially in the neighborhood of f^*, the WD mode is observed but suddenly disappears, and the CV(B) with very narrow roll

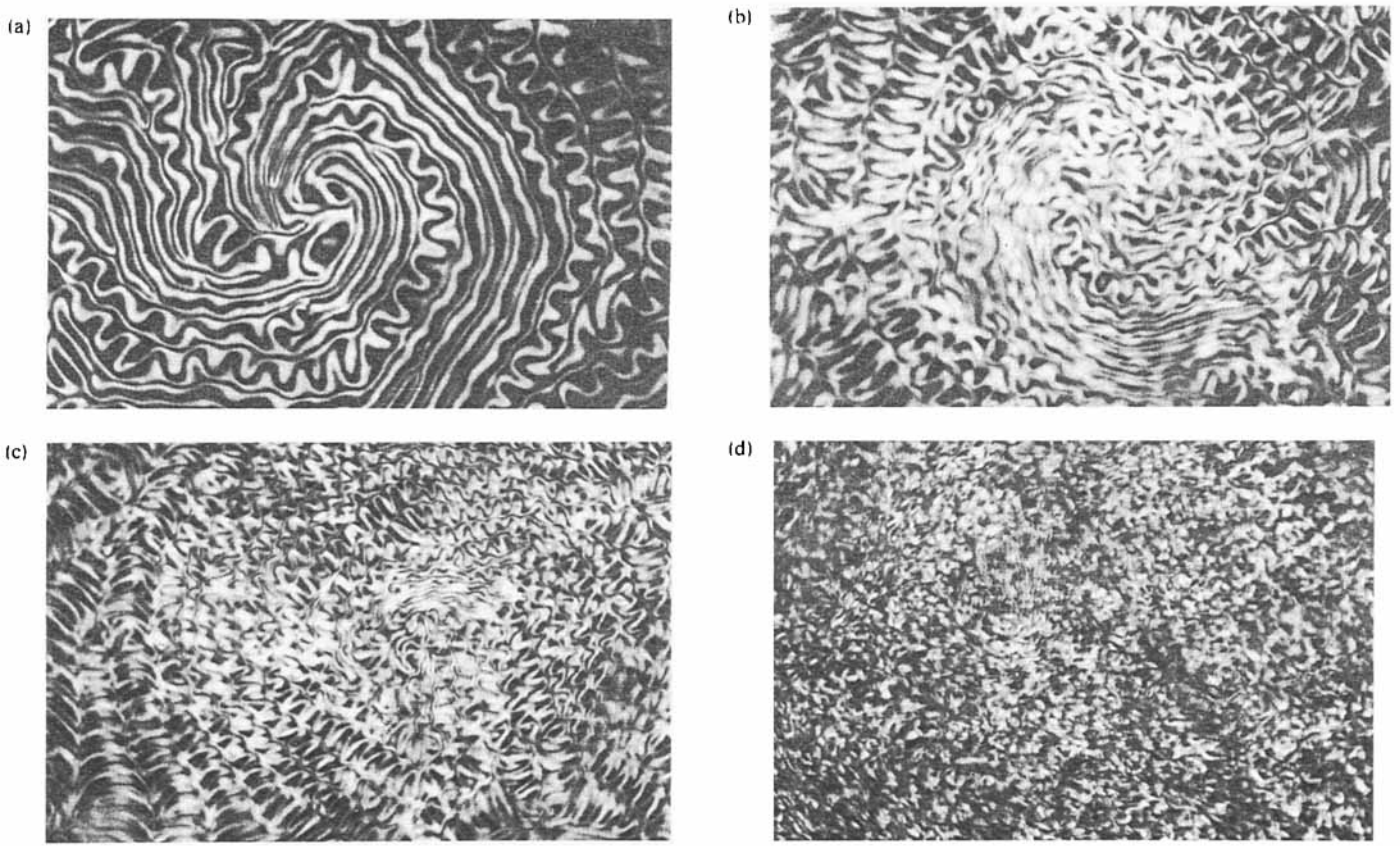

FIGURE 12 The patterns for $P^{**} < P < P^{*}$ (a) WP, (b) PWP1, (c) PWP2, (d) DSM.

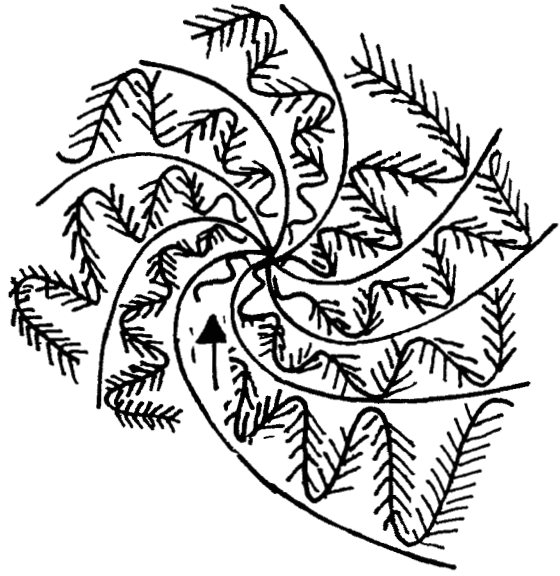

FIGURE 13 The detailed flow figure of the PWP. Along the wavy roll, the CV(B) is observed as shown in this schematic figure. The arrow shows the direction of the propagation of the wave.

width appears. When the WD is not observed (this case occurs frequently), a large scale macroscopic flow occurs before the CV(B) appears. It is of interest that an oscillating mode appears after the appearance of such an inhomogeneity. The characteristic patterns are shown in Figure 14. The CV(B), which is named CV(B)1, is an oscillating mode with extremely large wave number and becomes a distinct chevron texture with an increase of voltage. The transition from WD to CV(B) occurs sharply. In this CV-region, the characteristic propagation of a non-linear wave is recognized. In spite of the occurence of collisions among roll waves with opposite motion which comprises the CV(B), they pass through each other without stopping and mixing.

With further increase of voltage, the roll width of the chevron texture becomes half that of CV(B)1 and the chevron texture is seen in the WD-like pattern. The feature is noticeable in the case of applying a rectangular wave. This behavior closely resembles that in the double frequency region of an isotropic fluid. In the present study, this pattern is named the CV(B)2. The WD-like mode eddies with increase of voltage and bears a resemblance to PWP2. This mode is rotating and the pattern grows. However, as the voltage approaches the DSM-like point the flow with a moving closed-waist thread appears, then the CV pattern is destroyed. The flow of the CV(B) is shown in Figure 15. Here the WD mode and the chevron pattern propagate along

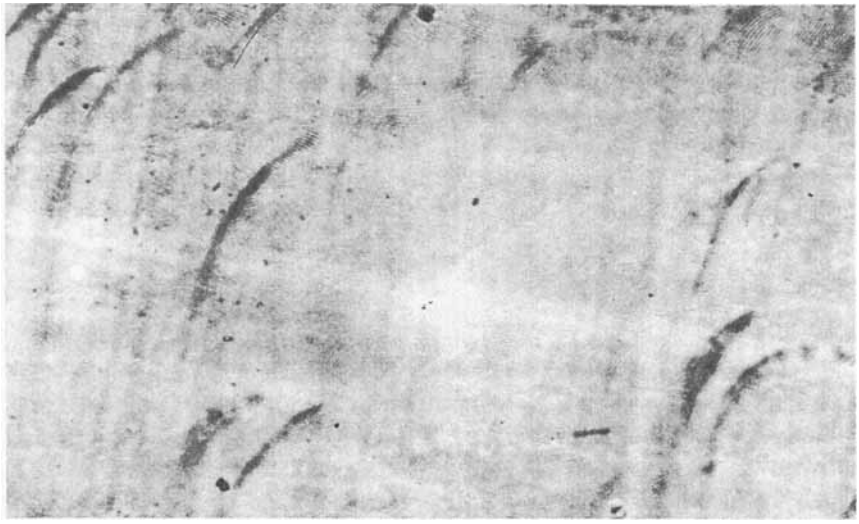

FIGURE 14 The CV(B). $f = 200$ Hz ($f_c = 56$ Hz). This pattern occurs in the phase diagram Fig. 1(b).

the WD-axis as shown by the arrows. In transverse observation, the propagation resembles that of the PWD but is small scale. In the WD mode, as shown in the figure by short arrows, adjacent lying CV(B) modes move in opposite directions to each other. Their points of contact are not seen clearly in a visual observation but very quickly a matching of flows should be achieved.

The schematic figure of the PWP is shown in Figure 13, which is formed in a low purity specimen. The existence of CV(B) patterns around the wavy

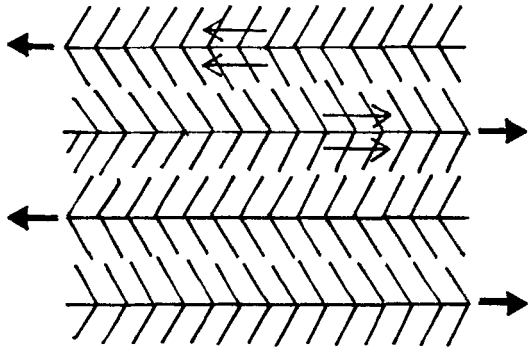

FIGURE 15 Schematic figure of the CV(B). The directions of motion of the pattern are shown by the arrows.

roll, shown in Figure 13, cannot be shown by photograph because of their high speed motion. In the PWP region, this propagation of a wavy pattern corresponds with the propagation along the WD-mode axis in the CV(B) pattern. Therefore, the propagation velocity of the wavy roll should show the same velocity as in the CV(B). The CV(B)1 and CV(B)2 correspond respectively to PWP1 and PWP2. The propagation of rolls is also shown by arrows in the figure.

5 $P < P^{**}$

In this region, no distinct spatial pattern is formed. Irregularly formed islands and a considerably large scale flow are seen at first. In the plane figure, it is seen that the moving closed-waist threads spring out: these threads could be formed by flow of the liquid crystal but the details are not clarified at present. When the voltage is increased, these threads grow in the space to become completely deformed, closed-waist ones and the system develops into a turbulent flow without forming a distinctly stationary pattern in the process. On the other hand, in the transverse figure the slowly

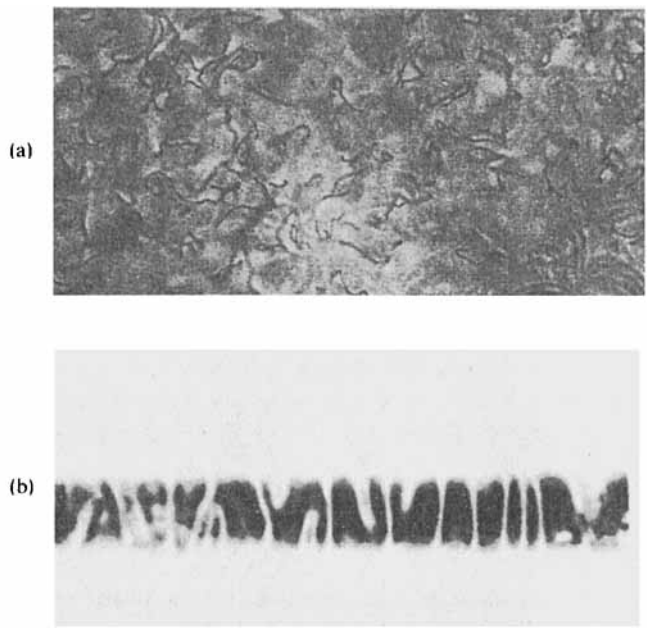

FIGURE 16 The walking line pattern. (a) Plane figure. (b) Transverse figure: this pattern propagates and is clearly different from the WD and the disclination.

trembling, fine threads propagate along the direction parallel to the electrodes. The threads extend between electrodes, nearly perpendicular to them. In the course of an increase of voltage, new threads appear from one electrode and contact with the nearest neighboring threads, forming U-typed threads or bending threads. The former diminishes frequently into the electrode. This feature is distinctly different from the transverse figures of the PWD and a disclination in the WD. These aspects are shown in Figure 16; we call this the walking line.

The position of P^{**} is well defined as a transition point. The thicker the cell, the more easily the observation of this region is made. On the other hand, in the thinner cell this region is not frequently observed because of the wide region of the CV(B). In this region a very high frequency is required and provided the cell is not broken, the phenomena can be generally observed even at a high voltage. A very highly dissipative structure would be realized as well as the vortex patterns in the WP and PWP. It is of great interest why a time-dependent flow without any stationary pattern occurs from the beginning as the limit of a electric Prandtl number. Here presumably a number of modes becomes unstable simultaneously. The turbulent flow exhibits a very large scale.

4 CONCLUSIONS

In the present study, we have reported the dissipative structures caused by convection in the nematic liquid crystal MBBA. It has been demonstrated that the phenomena caused by electrohydrodynamic effect bear a close resemblance to the Benard–Rayleigh problem in an isotropic fluid. At present, in the case of the isotropic fluid the following questions are not well clarified.

1) The property of the first appearing dissipative structure and bifurcation in a low Prandtl number fluid. A recent experiment by Krishnamurti for mercury shows that a time-dependent flow occurs from the beginning.[1] In this sort of experiment, it is difficult to clarify the phenomenon because direct observation of flow cannot be made.

2) The origin and the property of time-dependent flow.

3) The number of bifurcations to turbulent flow after a limit cycle first appears.

In the present study, the answers to some of these questions are obtained.

1) The first appearing visual pattern in a low Prandtl number fluid is the oscillating mode called the chevron texture. However, before this pattern

appears, an extremely large scale flow occurs. Therefore an instability occurs at finite amplitude of flow.

2) It is considered that several instabilities (more than two) occur simultaneously at the bifurcation point of the CV(B), where the CV(B) corresponds to the GP or the quasi-GP in the high region of P.

3) Two or three limit cycles appear during the approach to non-periodic flow. This result supports the Ruelle–Takens' theory.

Although the results obtained in the present study are less than quantitative, the transitions are distinctly caused by well-defined applied stress and various flow patterns have been obtained by changing the external parameters. However, by employing the discussion made in the present study, one can interprete the phenomena in isotropic fluids by appropriate comparison of parameters. Details will be reported elsewhere in the near future.[15]

Acknowledgements

We wish our hearty thanks to Professor K. Hashimoto and Mr. T. Hirano for their help with the microscopic observations and Dr. K. McNeil for reading the manuscript.

References

1. R. Krishnamurti, *J. Fluid Mech.*, **33**, 445, 457 (1968); *J. Fluid Mech.*, **42**, 295, 305 (1970); *J. Fluid Mech.*, **60**, 285 (1973).
2. J. B. McLaughlin and P. C. Martin, *Phys. Rev.*, **A12**, 186 (1975).
3. D. Coles, *J. Fluid Mech.*, **21**, 385 (1965).
4. For example, E. Dubois-Violette, P. G. de Gennes, and O. Parodi, *J. Phys.*, **32**, 305 (1971).
5. S. Kai, N. Yoshitsune, and K. Hirakawa, *J. Phys. Soc. Japan*, **40**, 267 (1976).
6. S. Kai, M. Araoka, H. Yamazaki, and K. Hirakawa, *J. Phys. Soc. Japan*, **40**, 305 (1976).
7. S. Kai and K. Hirakawa, *Solid State Comm.*, **18**, 1579 (1976).
8. S. Kai, K. Yamaguchi, and K. Hirakawa, *Japan. J. Appl. Phys.*, **14**, 1653 (1975).
9. S. Kai and K. Hirakawa, submitted to *Mol. Cryst. Liquid Cryst.*
10. T. Kai, S. Kai, and K. Hirakawa, *Tech. Rep. Kyushu Univ.*, **49**, 501 (1976).
11. S. Kai and K. Hirakawa, *J. Phys. Soc. Japan*, **40**, 301 (1976).
12. S. Kai and K. Hirakawa, *Solid State Comm.*, **18**, 1573 (1976).
13. W. S. Quon and E. Wiener-Avnear, *Solid State Comm.*, **15**, 1761 (1974).
14. F. H. Busse, *J. Fluid Mech.*, **52**, 97 (1972).
15. S. Kai and K. Hirakawa, *Mem. Fac. Engin. Kyushu Univ.*, (to be published).